Bioorganic & Medicinal Chemistry 18 (2010) 2141–2151

Contents lists available at ScienceDirect

Bioorganic & Medicinal Chemistry

journal homepage: www.elsevier.com/locate/bmc

Exploration of inhibitors for diaminopimelate aminotransferase

Chenguang Fan [a], Matthew D. Clay [b], Michael K. Deyholos [c], John C. Vederas [a,*,†]

[a] Department of Chemistry, University of Alberta, Edmonton, Alberta, Canada T6G 2G2
[b] St. Mary's University College, 14500 Bannister Road SE, Calgary, Alberta, Canada T2X 1Z4
[c] Department of Biological Sciences, University of Alberta, Edmonton, Alberta, Canada T6G 2E9

ARTICLE INFO

Article history:
Received 30 November 2009
Revised 31 January 2010
Accepted 2 February 2010
Available online 6 February 2010

Keywords:
Lysine biosynthesis
Aminotransferase
Diaminopimelate (DAP)
Arabidopsis thaliana
Pyridoxal-5′-phosphate (PLP)
Chlamydia
Enzyme inhibition

ABSTRACT

Bacteria and higher plants make L-lysine from diaminopimelic acid (DAP). In mammals L-lysine is an essential amino acid that must be acquired from the diet as the biosynthetic pathway is absent for this key constituent of proteins. Recently, LL-diaminopimelate aminotransferase (LL-DAP-AT), a pyridoxal-5′-phosphate (PLP)-dependent enzyme, was reported to catalyze a key step in the route to L-lysine in plants and *Chlamydia*. Specific inhibitors of this enzyme could thus potentially serve as herbicides or antibiotics that are non-toxic to mammals. In this work, 29,201 inhibitors were screened against LL-DAP-AT and the IC_{50} values were determined for the top 46 compounds. An aryl hydrazide and rhodanine derivatives were further modified to generate 20 analogues that were also tested against LL-DAP-AT. These analogues provide additional structure–activity relationships (SAR) that are useful in guiding further design of inhibitors.

1. Introduction

Lysine biosynthesis occurs via the diaminopimelate (DAP) pathway in both plants and bacteria, but is absent in mammals, which acquire this essential amino acid in their diet. It is believed that effective inhibitors of enzymes in the DAP pathway would be non-toxic to humans but could act as potent herbicides or antibiotics. This has prompted numerous reviews[1–4] and continuing studies on both the structures of the protein catalysts[5–11] as well as design of inhibitors[12–15] since the mid 1980s.[16] Lysine is often the limiting amino acid in the human diet, and thus a complete understanding of its biosynthetic route would also assist engineering of plants with increased lysine content for better nutrition.[17]

In most bacteria, the DAP pathway (Fig. 1a) begins with the condensation of L-aspartate semialdehyde with pyruvate in the presence of DHDP synthase to form L-dihydrodipicolinate (DHDP), which is then reduced to L-tetrahydrodipicolinate (THDP) by DHDP reductase. THDP is then converted to LL-diaminopimelic acid (LL-DAP) through N-succinylation, transamination, and desuccinylation by the actions of THDP acyltransferase, *N*-acyl-DAP aminotransferase, and *N*-acyl-DAP deacylase, respectively.[4] LL-DAP is epimerized to *meso*-DAP by DAP epimerase[18,19] and finally transformed into L-lysine by DAP decarboxylase. This pathway was also thought to be present in higher plants until 2006 when Gilvarg, Leustek and co-workers found that an alternative shorter route is used in higher plants and cyanobacteria for L-lysine biosynthesis.[20] The new route is similar to the bacterial pathway; however, L-THDP is converted to LL-DAP by a single enzyme, LL-DAP aminotransferase (LL-DAP-AT) (Fig. 1b), bypassing three enzymatic steps present in bacteria. As in the bacterial path, LL-DAP is then converted to *meso*-DAP by DAP epimerase[6] and decarboxylated[21] to yield L-lysine. Recently, the crystal structure of LL-DAP-AT from *Arabidopsis thaliana* was obtained by our group, and the mechanism of substrate recognition and pyridoxal-5′-phosphate (PLP)-induced conformational changes in LL-DAP-AT were examined.[7,22] In this transamination, L-glutamate is used as the amino donor and the reaction occurs via the typical PLP mechanism. The LL-DAP-AT pathway is also shared by *Chlamydia trachomatis* and *Protochlamydia amoebophila*.[23] Chlamydiae are known to cause many diseases in both humans and animals, including sexually transmitted infections, infectious blindness (*C. trachomatis*), coronary heart disease, and atherosclerosis (*C. pneumoniae*), along with a variety of diseases in poultry and livestock (*Chlamydophila*).[23] Recent genetic analysis has shown that LL-DAP-AT occurs in *Cyanobacteria*, *Desulfuromonadales*, *Firmicutes*, *Bacteroidetes*, *Chlamydiae*, *Spirochaeta*, and *Chloroflexi* and two archaeal groups, *Methanobacteriaceae* and *Archaeoglobaceae*.[24,25]

Abbreviations: DAP, 2,6-diaminopimelic acid; DAP-AT, diaminopimelate aminotransferase; DHDP, dihydrodipicolinic acid; 2-OG, 2-oxoglutarate; OAB, 2-aminobenzaldehyde; PLP, pyridoxal phosphate; SAR, structure–activity relationship; THDP, tetrahydrodipicolinic acid.

* Corresponding author. Tel.: +1 780 492 5475; fax: +1 780 492 2134.
E-mail address: john.vederas@ualberta.ca (J.C. Vederas).
† Canada Research Chair in Bioorganic and Medicinal Chemistry.

0968-0896/$ - see front matter © 2010 Elsevier Ltd. All rights reserved.
doi:10.1016/j.bmc.2010.02.001

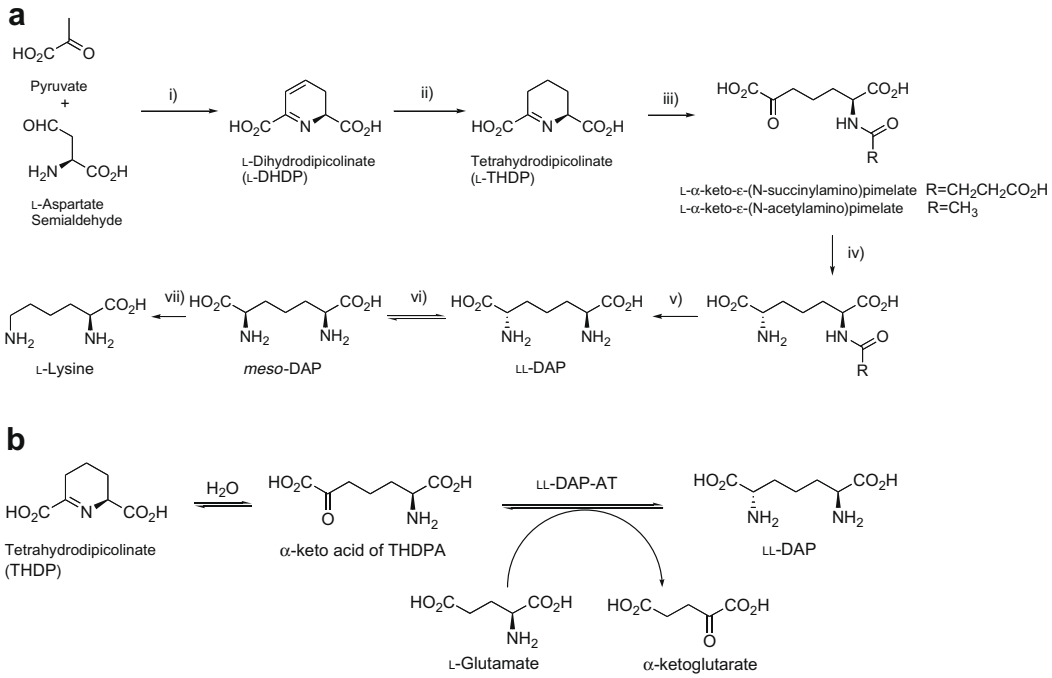

Figure 1. (a) L-Lysine biosynthesis via DAP pathway in bacteria. Reagents: (i) DHDP synthase; (ii) DHDP reductase; (iii) THDP acyltransferase; (iv) *N*-acyl-DAP aminotransferase; (v) *N*-acyl-DAP deacylase; (vi) DAP epimerase; (vii) DAP decarboxylase. (b) The shortcut of DAP pathway in plants and *Chlamydiae*.

In certain cases, compounds that inhibit DAP enzymes have already been shown to have antimicrobial activity.[3,12,26] It thus seemed that inhibitors that directly target LL-DAP-AT could be applied as herbicides or new antibiotics specific for *Chlamydiae*. Rational design of inhibitors of enzymes in the DAP pathway that are based on corresponding substrates can be very effective, but their antibiotic activity is often compromised by poor uptake by bacterial cells.[3] Hence, in this study a library of 29,201 accessible drug-like compounds were robotically screened for inhibition of LL-DAP-AT. The top 46 candidates were subjected to IC_{50} determination. Finally, preliminary structure–activity relationship (SAR) studies were done based on modification of two lead structures, a hydrazide and a rhodanine.

2. Results and discussion

The initial 29,201 compounds were obtained from ChemBridge Corporation. LL-DAP-AT from *A. thaliana* was cloned and overexpressed in *Escherichia coli* with a C-terminal hexahistidine tag to aid in protein purification, as previously reported.[7,22] A known 2-aminobenzaldehyde (OAB)-based assay[20] (Fig. 2) was adapted to function reliably in a 96-well plate. The eight wells of column 1 of the 96-well plate served as a positive control (no inhibitor), whereas column 12 served as a negative control (no enzyme). The initial and final absorbance at 440 nm of each well was measured using an automated spectrophotometer, and the difference was used as an indicator of enzyme activity. Activity was determined relative to the average of column 1 (positive control). The assay procedure consisted of four steps and was done using an automated workstation as described in the experimental section. The percentage inhibition was determined at a concentration of 10 μM for all of the inhibitors (an estimated molecular weight of 500 g/mol was assumed for each inhibitor candidate when calculating the concentration in this robotic screening).

After robotic screening of the 29,201 compounds, the top 46 compounds were selected for further manual testing and analysis. These substances displayed inhibition greater than 13% at 10 μM concentration in both robotic screening and manual testing, and thus were considered to be potentially good inhibitors. The IC_{50} value was measured manually using a UV–vis spectrophotometer. Both robotic and manual testing results are listed in Table 1. An interesting feature is that a high percentage of the compounds with good inhibitory activity contain a 'barbiturate' or 'thiobarbiturate' ring (compounds **B-1** to **B-16**). Within the 29,201 compounds, approximately 1000 compounds (~3%) possessed a moiety of this type, whereas 16 of the top 46 compounds (~35%) contained one of these groups as a potential pharmacophore.

The best inhibitor was found to be **C-1**, with an IC_{50} of 5 μM. However, this compound contains a hydrazide functionality having a free NH_2, a group that is well known to react readily with PLP.

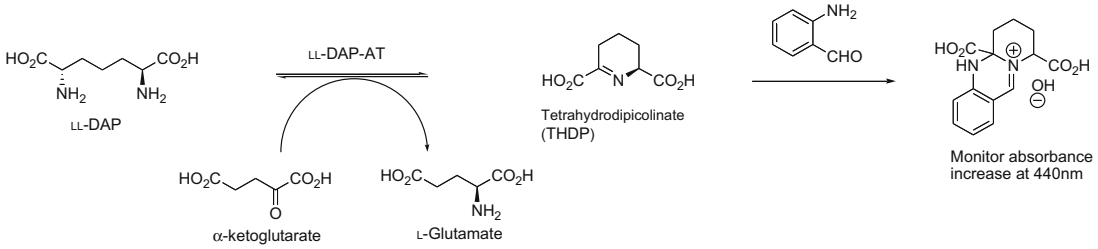

Figure 2. Testing method for inhibitor against LL-DAP-AT.

Table 1
Testing results

Entry	Structure	%Inhibition[a]/IC_{50} (μM)[b]	Entry	Structure	%Inhibition[a]/IC_{50} (μM)[b]
A-1	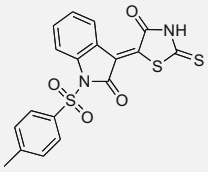	25 70	**A-2**	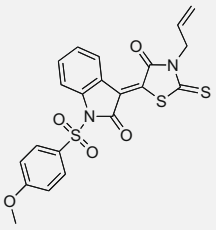	18 194
A-3	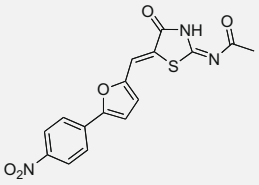	52 78	**A-4**	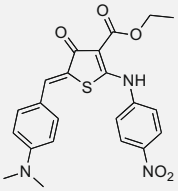	19 141
A-5	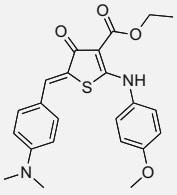	22 >200	**A-6**	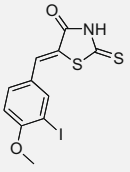	29 180
A-7	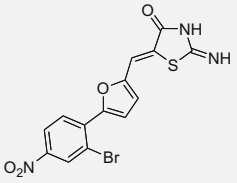	13 85	**A-8**	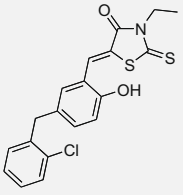	13 46
A-9	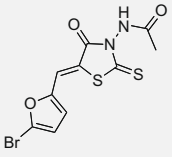	13 41[c]	**A-10**	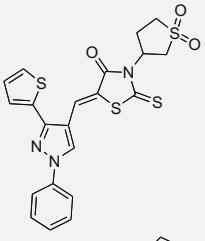	13 117
A-11	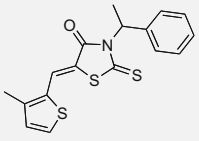	13 127	**A-12**	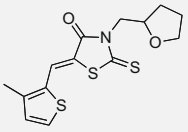	14 >200
A-13	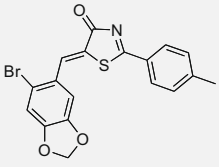	13 130	**B-1**	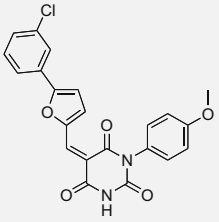	20 42
B-2	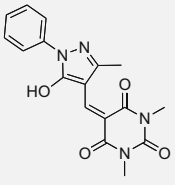	20 45[c]	**B-3**	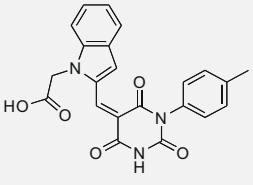	17 37

(*continued on next page*)

Table 1 (*continued*)

Entry	Structure	%Inhibition[a]/IC_{50} (μM)[b]	Entry	Structure	%Inhibition[a]/IC_{50} (μM)[b]
B-4	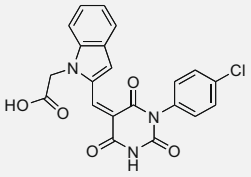	14 65	**B-5**	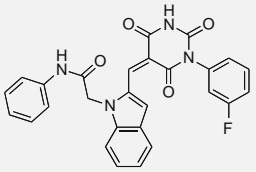	18 52
B-6	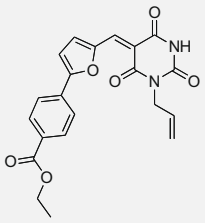	16 >200	**B-7**	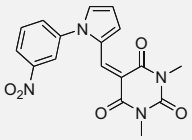	13 >200
B-8	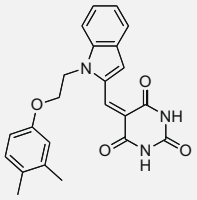	28 99	**B-9**	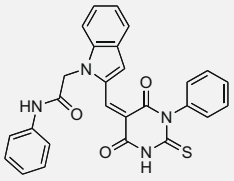	45 33[d]
B-10	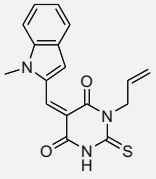	35 75	**B-11**	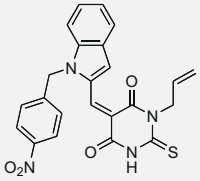	33 69
B-12	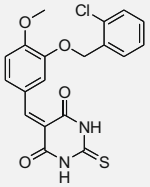	48 121	**B-13**	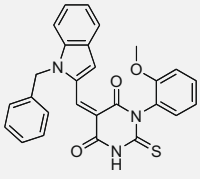	20 62
B-14	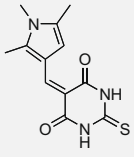	15 25[c]	**B-15**	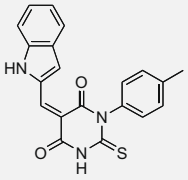	16 164
B-16	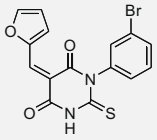	17 >200	**C-1**	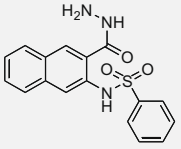	33 5[c]
C-2	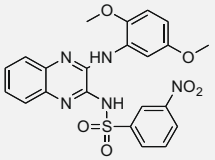	13 153	**C-3**	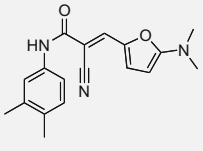	14 >200
C-4	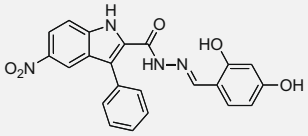	15 45	**C-5**	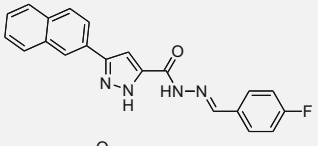	14 161
C-6	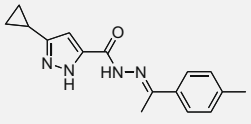	14 >200	**C-7**	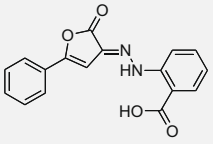	16 39[c]

Table 1 (*continued*)

Entry	Structure	%Inhibition[a]/IC_{50} (μM)[b]	Entry	Structure	%Inhibition[a]/IC_{50} (μM)[b]
C-8	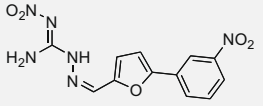	13 >200	**C-9**	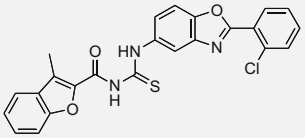	19 83
C-10	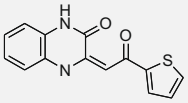	15 31	**C-11**	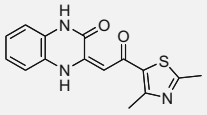	18 56
C-12	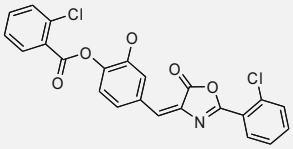	30 81	**C-13**	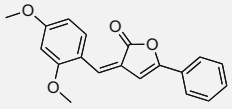	14 159
C-14	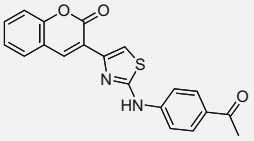	16 >200	**C-15**	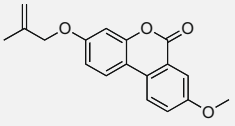	25 >200
C-16	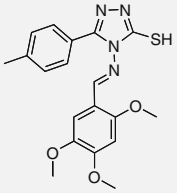	18 >200	**C-17**	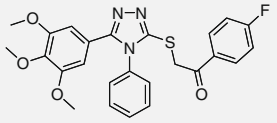	14 >200

[a] Robotic screening at inhibitor concentration of 10 μM.
[b] Manually tested for IC_{50} value.
[c] Time-independent type inhibitor (competitive, non-competitive, or uncompetitive).
[d] Time-dependent type inhibitor (affinity label, mechanism-based irreversible inactivation, or slow-binding).

Thus, even though the compound **C-1** shows high potency and time-independent inhibition, this may be due to reaction of the compound with PLP, rather than with the LL-DAP-AT enzyme. Based on preliminary kinetic studies, compound **C-1** appears to be an uncompetitive inhibitor of LL-DAP-AT. Two analogues of **C-1** were also synthesized in which the hydrazine moiety was masked (Scheme 1). In compound **2**, the free hydrazide terminus was masked by a six-membered ring, which would decrease the nucleophilicity but retain the basicity of the nitrogen atom. In compound **3**, the amino group was acetylated to decrease both the nucleophilicity and basicity of the nitrogen. Upon testing, it was shown that neither analogue was an inhibitor of LL-DAP-AT, suggesting that the inhibitory effect of compound **C-1** may be at least partly due to the reaction of the hydrazide amino group with PLP. We therefore focused our initial efforts on other good inhibitors identified by screening. However, it should be noted that

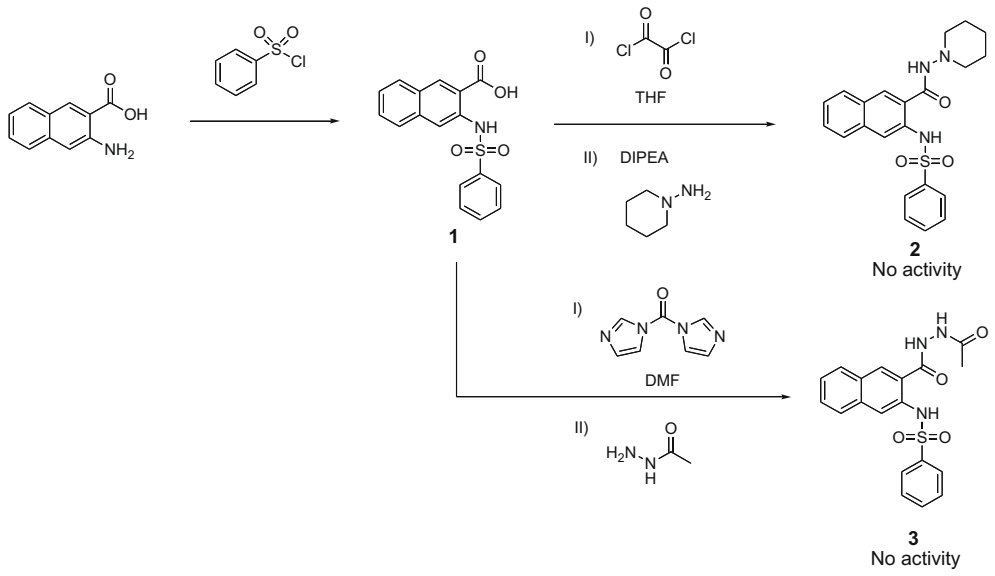

Scheme 1. Preparation and testing results of the analogues for compound **C-1**.

certain useful drugs, for example, the antituberculosis agent isoniazid,[27] possess such an unsubstituted hydrazide on an aromatic ring.

The initial objective was to find inhibitors that displayed time-independent behavior and interacted reversibly only with the enzyme. A number of inhibitors exhibited IC_{50} values of 20–60 μM, and as mentioned above, a significant percentage of these contained barbiturate and thiobarbiturate moieties with a conjugated exocyclic double bond. Similar barbiturate-based compounds have been studied extensively in the past, and have been shown to be good methionine aminopeptidase-1 inhibitors,[28] as well as potent inhibitors of metalloenzymes.[29] However, such unsaturated barbiturate derivatives can be expected to be good Michael acceptors and may react with nucleophilic groups on the enzyme to form covalent bonds. Hence they would not be time-independent reversible inhibitors and would have the potential to react with other biomolecules, which could lead to mammalian toxicity. Preliminary testing of these compounds as inhibitors of LL-DAP-AT revealed that most, such as **B-9**, were time-dependent inhibitors, suggesting a non-reversible reaction of the inhibitor with the enzyme or a slow-binding inhibition. Although a few barbiturate-based candidates, such as compounds **B-2** and **B-14**, did show time-independence, and preliminary kinetic studies suggest that **B-14** shows uncompetitive inhibition, we chose to initially exclude barbiturate-based compounds from the current work to avoid complications arising from their ability to behave as Michael type acceptors.

In this study, the rhodanine-based inhibitors (**A-1** to **A-13**) were selected for further investigation because there were no obvious functional groups reactive toward PLP or the enzyme, and thus these compounds were more likely to be time-independent type inhibitors. However, within this group of inhibitors, the inhibitory activity was not particularly high and trends in SAR studies were unclear. Fortunately, the synthesis of these types of compounds was straightforward and allowed for facile preparation of analogues. The top two inhibitors, **A-8** and **A-9**, with IC_{50} values of 46 and 41 μM, respectively, were shown to be time-independent type inhibitors, and were chosen to be the two lead compounds. The substituents on both of the nitrogens of the rhodanine ring and on the aromatic ring were varied in this preliminary study.

The route used to synthesize the analogues is shown in Scheme 2, and the results for the inhibition testing are listed in Table 2. The data show that no analogue exhibited better inhibition than the lead compounds. However, several conclusions can be drawn that are useful in guiding further study. Substitution on the nitrogen of the rhodanine ring does not appear to have a significant effect on the inhibitory potency of the compound as two of the best analogue inhibitors (**4c** and **4d**) possessed only a hydrogen atom on the nitrogen. Furthermore, comparison of analogues in which only the substituent on nitrogen was varied (e.g., [**4a**, **5a**, **6a**, **7a**], [**4b**, **5d**, **6c**, **7c**], or [**4d**, **5c**, **6b**, **7b**]) does not reveal any significant differences. Although the tested substituents are of somewhat different size, it is perhaps more surprising to note the absence of any electronic effect despite the dramatically different electronic properties of amino and *N*-acetyl substituents. These results imply that the substituent on the rhodanine does not dramatically affect activity. Comparison of analogues in which the substituent on nitrogen was kept the same while the substituents on the aromatic ring were varied reveals that an electron-donating group (e.g., $-OCH_3$) on the aromatic ring increases the activity of the inhibitor (e.g., [**4a**, **4d**], [**5a**, **5c**], [**6a**, **6b**], [**7a**, **7b**]). This effect is most pronounced for those analogues in which the nitrogen substituent is either a hydrogen or an amino group. Replacement of the $-OCH_3$ group with a slightly electron-withdrawing chlorine atom (e.g., **4b**, **5b**, **6c**, **7c**) results in a drop in activity in three of the four examples. The location of the substituent also appears to play a role, as an electron-donating substituent (–OH) added to the *ortho* position (**4g**) decreases the inhibition compared to **4d**, although it is still better than the unsubstituted ring. Interestingly, the most potent analogue (**7d**) is substituted with a furan ring instead of a benzene ring, as in the case of lead compound **A-8**. Similar to **A-9**, compound **7d** also possesses an electron-withdrawing substituent in the 5-position of the furan ring, albeit a substantially larger one.

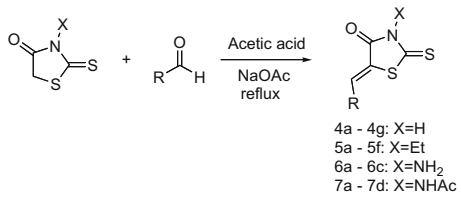

Scheme 2. General reaction for the synthesis of rhodanine-based inhibitors.

Three of the best inhibitors were chosen for preliminary general antimicrobial activity testing in vitro. The inhibitors examined were **B-14**, **C-1**, and **C-7**, which had IC_{50} values with LL-DAP-AT of 25, 5, and 39 μM, respectively. As expected, none of these inhibitors showed antimicrobial activity at concentrations lower than 200 μg/mL in preliminary tests against *E. coli* DH5α, *Pseudomonas aeruginosa* ATCC 15442, *Salmonella typhimurium* ATCC 23564, *Staphylococcus aureus* ATCC 25923, and *Carnobacterium divergens* LV13. However, these organisms do not use LL-DAP-AT in their biosynthetic pathway to L-lysine. Studies targeted against plants and *Chlamydia*, both of which do use LL-DAP-AT, will be reported in the future.

3. Conclusions

In this study, 46 compounds displaying greater than 13% inhibition (at 10 μM) of LL-DAP-AT, were identified from a compound library of 29,201, using robotic screening. Fifteen of these 46 compounds had IC_{50} values of 60 μM or lower. Of the 46 compounds, 13 possessed a rhodanine moiety, whereas 16 had a barbiturate or thiobarbiturate moiety, suggesting potential pharmacophores. The best inhibitor is hydrazide **C-1**, with an IC_{50} value of 5 μM. However, it is likely that this is at least partly due to reaction with the PLP co-factor, rather than direct inhibition of the target enzyme. The rhodanine-based inhibitors were chosen as lead compounds for SAR studies. Upon analysis of the results, it appears that the substituent on the nitrogen has little effect on the activity of these inhibitors, whereas the presence of an electron-donating group on the aromatic ring enhances activity. Several compounds were also found to be good inhibitors aside from the compounds mentioned above. Compounds **C-4**, **C-7**, **C-10**, and **C-11** had IC_{50} values of 45, 39, 31, and 56 μM respectively. In the future, additional analogues can be synthesized based on these compounds, and also on aryl hydrazide **C-1**, as possible inhibitors of LL-DAP-AT with useful antimicrobial or herbicidal activity.

4. Experimental

4.1. Inhibitor screening

4.1.1. Aliquot buffer solution to 30 plates

420 mg of 2-oxoglutarate (2-OG), 280 mg 2-aminobenzaldehyde (OAB), and 480 mg of racemic DAP were dissolved in 280 mL of 100 mM HEPES-KOH, pH 7.6, and 85 μL of this stock was aliquoted to empty 96-well assay plates using an automated protocol on a Beckman Coulter Biomek 2000 Laboratory Automation Workstation. The final concentration of each component in the stock solution is: 2-OG (10 mM); OAB (8.3 mM); LL-DAP (assuming 25% of total DAP: 2.3 mM). Upon dilution to 100 μL in the well plate, the final concentrations are: 2-OG (8.5 mM); OAB (7 mM); LL-DAP (2.0 mM).

Table 2
Testing results for rhodanine-based analogues

Entry	X	R	IC_{50} (μM)	Entry	X	R	IC_{50} (μM)
4a	H		No activity	**4b**	H	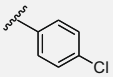	>200
4c	H	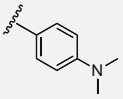	127	**4d**	H	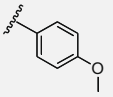	142
4e	H		No activity	**4f**	H		No activity
4g	H		>200				
5a	Et		>200	**5b**	Et		>200
5c	Et	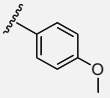	>200	**5d**	Et	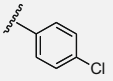	~200
5e	Et		~200	**5f**	Et		190
6a	NH_2		No activity	**6b**	NH_2	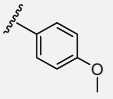	155
6c	NH_2	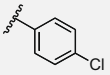	No activity				
7a	NHAc		No activity	**7b**	NHAc	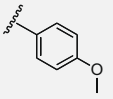	>200
7c	NHAc	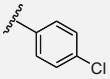	No activity	**7d**	NHAc	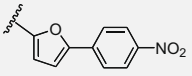	73

4.1.2. Preparation of inhibitor working stock

The inhibitor source plates contained 0.25 mg of inhibitor in 25 μL of DMSO. Inhibitor was present in columns 2–11 of 96-well plates; columns 1 and 12 contained pure DMSO. Using an automated protocol on the Biomek 2000, 99 μL of DMSO was added to each well of a 96-well plate, followed by 1.0 μL of inhibitor to create the inhibitor working stock. Assuming a molecular weight of 500 g/mol, the final concentration of inhibitor in each well is 200 μM. The working plates were stored at −20 °C.

4.1.3. Addition of inhibitor

A 5 μL solution of inhibitor working stock was then added to the assay plates containing buffer using an automated protocol on the Biomek 2000. Columns 1 and 12 of the assay plates received pure DMSO as no inhibitor was present in these columns in the inhibitor source plates. Assuming a molecular weight of 500 g/mol, the final concentration of inhibitor in each well is 10 μM. In a few cases, there were inhibitor solubility problems, but these tests were discarded in the interest of high throughput. To remove air bubbles, the assay plates were then centrifuged at 2400 rpm for 3 min. The absorbance was then recorded at 440 nm in triplicate on a Bio-TEK PowerWave XS Universal Microplate Spectrophotometer.

4.1.4. Addition of enzyme

A 0.043 mg/mL solution of LL-DAP-AT in 100 mM HEPES-KOH pH 7.6 was prepared and 10 μL of this was added to each well (with the exception of column 12, which served as a negative control) using an automated protocol on the Biomek 2000. This resulted in 0.43 μg of enzyme in each well, or a concentration of 0.0043 mg/mL of LL-DAP-AT. The assay plates were then allowed to sit at room temperature for 3 h, at which time a second absorbance reading at 440 nm was taken in triplicate.

4.2. Determination of IC_{50}

4.2.1. Aliquot buffer solution

420 mg of 2-oxoglutarate and 480 mg of racemic DAP (commercial) were dissolved in 280 mL of 100 mM HEPES-KOH, pH 7.6. Seven milliliters of this solution were used to dissolve 7 mg of 2-aminobenzaldehyde (OAB) and 850 μL of this stock was added into eight assay cells (1 mL). The final concentration of each component in the stock solution is: 2-OG (10 mM); OAB (8.3 mM); LL-DAP (assuming 25% of total DAP: 2.3 mM). Upon dilution to 1 mL in the assay cells, the final concentrations are: 2-OG (8.5 mM); OAB (7 mM); LL-DAP (2.0 mM).

4.2.2. Preparation of inhibitor working stock

Eight micromoles of inhibitor were dissolved in 2 mL of DMSO, which resulted 4 μmol/mL in concentration. The serial dilution gave 2, 1, 0.5, 0.2, and 0.1 μmol/mL solutions. In the final assay cell, the inhibitor concentrations were 200, 100, 50, 25, 10, and 5 μM, respectively.

4.2.3. Addition of inhibitor

Fifty microliters of each concentration of inhibitor solutions were added into cell 2–7. And 50 μL of pure DMSO was added into cell 1 and 8, which are control and negative control. The Varian Cary 100 Bio UV–Visible spectrophotometer was used to measure the absorbance at 440 nm. Under the program of Enzyme Kinetics the absorbance for all the cells were then multi-zeroed.

4.2.4. Addition of enzyme

A 0.043 mg/mL solution of LL-DAP-AT in 100 mM HEPES-KOH pH 7.6 was prepared and 100 μL of this was added to each cell, except the negative control (cell 8). The final concentration of the enzyme was 0.0043 mg/mL. The absorbance was recorded for 200 min with 2 min/cycle. The initial rate of increase of the absorbance is proportional to the rate of reaction. By comparing the initial slope of each absorbance curve of the inhibitor assay cell to the control cell, the percentage inhibition was determined and the IC_{50} value was calculated based on this data.

4.3. Time dependent/independent testing

The concentration of inhibitor stock was chosen, based on the IC_{50} value determined. The substrate buffer solution and the enzyme were prepared, as described above. Six portions of 100 μL of enzyme and 50 μL of inhibitor solution were pre-incubated for different lengths of time before addition into the cell, containing 850 μL of substrate buffer solution. Cells 1 and 8 served as positive and negative control, respectively. The absorbance was recorded as described above. For the time-independent inhibitors, the percentage inhibition did not change with different incubation times. For the time-dependent inhibitors, the percentage inhibition increased with longer pre-incubation times.

4.4. Type of inhibition testing

Preliminary testing was carried out according to the description by Segel.[30] The concentration of inhibitor stock was chosen, based on the IC_{50} value determined. The concentration of LL-DAP was varied from 125 μM to 5 mM. The UV absorbance was monitored at 30 °C using a Spectra Max 340PC microplate reader controlled with SOFTmax® PRO software (Molecular Devices, Sunnyvale, CA) in the kinetics read mode. The wavelength was set at 440 nm and each well was monitored at 30 s intervals for up to 2 h. Data were then graphed and analyzed using GraphPad Prism® Version 4. For Michelis–Menten plots, a non-linear regression fit was employed. Data were transformed as a Lineweaver–Burk (double reciprocal) plot.

4.5. Preliminary antimicrobial testing

Ten milliliters of sterile, soft agar (0.75% w/v agar) containing the appropriate growth media (Luria Bertani for Gram-negative bacteria and M17 for Gram-positive bacteria) were heated in boiling water, until molten. After cooling to touch, the soft agar was inoculated with an overnight culture of the indicator organism (1%) and overlaid on a bed of solid agar (1.5% w/v agar). Solutions to be tested, including appropriate controls (acetonitrile for **C-1**, methanol for **B-14** and **C-7**), were spotted (10 μL) onto the agar and allowed to air dry. Plates were incubated overnight at the appropriate temperatures (37 °C for Gram-negative bacteria and 30 °C for Gram-positive bacteria) and examined for halos of growth inhibition.

4.6. Chemical preparation of analogues

All chemicals and solvents used in this study were purchased from Sigma–Aldrich and TCI. Infrared spectra were obtained using Nicolet Magna 750 FTIR Spectrometer and Nic-Plan FTIR Microscope. Varian Inova 300 MHz, 400 MHz, and Varian Mercury 400 MHz two-channel spectrometers were used to acquire ^1H and ^{13}C NMR spectra. Chloroform-D and DMSO-d_6 were used as NMR solvents. Spin multiples are listed as s (singlet), d (doublet), t (triplet), q (quartet), m (multiplet), and br (broad) and coupling constant (J) values were estimated in hertz (Hz). High-resolution mass spectra were obtained using Applied BioSystems Mariner BioSpectrometry Workstation (orthogonal acceleration Time-of-Flight, positive and negative ion ESI and APCI, Foster City, CA) and Kratos MS50G (positive ion EI).

4.6.1. 3-(Phenylsulfonamido)-2-naphthoic acid (1)

3-Amino-2-naphthoic acid (80%, 0.468 g, 2.00 mmol) and sodium carbonate (0.515 g, 4.80 mmol) were mixed with distilled water (5 mL). The mixture was heated in an oil-bath to ~60 °C. Benzenesulfonyl chloride (0.31 mL, 2.4 mmol) was slowly added into the mixture over the course of 15 min. The mixture was then heated to 85 °C for a further 2 h. Norite (20 mg) was added into the dark red mixture. The hot mixture was filtered through a pre-heated funnel. The filtrate was slowly added with vigorous swirling into a 50 mL flask, which contained of 6 N hydrochloric acid (1 mL). A red solid formed. The solid was filtered and washed with of 1 N hydrochloric acid (2 mL). The product (0.606 g, 93%) was a light red solid and was used directly. IR (Microscope) 3221, 3070, 2861 (br), 1676, 1448, 1160 cm^{-1}; ^1H NMR (400 MHz, DMSO-d_6): δ = 8.59 (s, 1H), 7.97 (d, J = 7.5, 1H), 7.91 (s, 1H), 7.89 (d, J = 7.5, 1H), 7.82 (m, 2H), 7.59 (m, 2H), 7.48 (m, 3H); ^{13}C NMR (100 MHz, DMSO-d_6): δ = 170.34, 139.26, 135.90, 135.70, 134.33, 134.13, 130.24, 130.08, 129.82, 129.22, 127.68, 127.62, 126.62, 118.25, 116.60; ESI-HRMS m/z calcd for $C_{17}H_{13}NO_4S$: 326.04925 [M+H^+], found: 326.04881.

4.6.2. 3-(Phenylsulfonamido)-*N*-(piperidin-1-yl)-2-naphthamide (2)

3-(Phenylsulfonamido)-2-naphthoic acid (0.0818 g, 0.250 mmol) was dissolved in dry THF (5 mL). The solution was cooled in an ice-bath, after 10 min, oxalyl chloride (28 μL, 0.32 mmol) was added. Then two drops of DMF were added into the mixture. The mixture was stirred for 30 min before being allowed to warm to 20 °C. The mixture was stirred for a further one hour. The solvent and excess oxalyl chloride was removed in vacuo. Dry THF (5 mL) was then added to the residue. *N,N*-Diisopropylethylamine (0.3 mL, 1.7 mmol) was added, followed by slow addition of 1-aminopiperidine (0.054 mL, 0.50 mmol). The mixture was stirred for 16 h, and then the solvent was removed in vacuo. The residue was dissolved in ethyl acetate (10 mL), and washed with saturated sodium bicarbonate solution (2 × 15 mL), water (15 mL), and brine (15 mL). The organic layer was dried over sodium sulfate followed by solvent removal in vacuo. The product was purified by column chromatography and yielded a white solid (0.073 g, 68%); R_f = 0.45 (2:1 ethyl acetate/hexanes); IR (Microscope) 3221, 3070, 2861 (br), 1676, 1448, 1160 cm^{-1}; ^1H NMR (400 MHz, $CDCl_3$): δ = 10.42 (br, 1H), 8.04 (s, 1H), 7.94 (br, 1H), 7.89 (d, J = 7.6 Hz, 2H), 7.72 (t, J = 8.0 Hz, 2H), 7.50 (t, J = 8.0 Hz, 2H), 7.36 (m, 3H), 2.84 (br, 4H), 1.76 (br, 4H), 1.47 (br, 2H); ^{13}C NMR (100 MHz, $CDCl_3$): δ = 166.87, 139.90, 135.10, 134.41, 132.91, 129.36, 129.13, 128.82, 128.59, 128.48, 127.70, 127.41, 126.25, 122.13, 119.06, 57.04, 25.29, 23.23; ESI-HRMS m/z calcd for $C_{22}H_{23}N_3O_3S$: 432.13523 [M+Na^+], found: 432.13481.

4.6.3. *N*-(3-(2-Acetylhydrazinecarbonyl)naphthalen-2-yl)benzenesulfonamide (3)

3-(Phenylsulfonamido)-2-naphthoic acid (0.0818 g, 0.250 mmol) and carbonyldiimidazole (0.041 g, 0.25 mmol) were dissolved in dry DMF (5 mL). The mixture was stirred for one hour.

Acetohydrazide (0.025 g, 0.30 mmol) was dissolved in DMF (1 mL) and was added to the mixture. The reaction was allowed to stir for 16 h at 20 °C. The solvent was then removed in vacuo, and the residue was dissolved in ethyl acetate (20 mL). The solution was washed with 10% citric acid (2 × 20 mL), saturated sodium bicarbonate solution (2 × 20 mL), water (20 mL), and brine (20 mL). The organic layer was dried over sodium sulfate, and solvent was removed in vacuo. The product was purified by column chromatography to yield a white solid (0.070 g, 73%); R_f = 0.28 (100% ethyl acetate); IR (Microscope) 3267, 3225, 3020, 1698, 1412, 1156 cm^{-1}; ^1H NMR (400 MHz, DMSO-d_6): δ = 10.73 (s, 2H), 10.08 (s, 1H), 8.28 (s, 1H), 7.84 (m, 5H), 7.53 (m, 5H), 1.99 (s, 3H); ^{13}C NMR (100 MHz, DMSO-d_6): δ = 169.42, 167.97, 139.17, 134.85, 134.34, 134.04, 130.52, 130.14, 129.69, 129.21, 129.14, 127.84, 127.67, 126.88, 121.08, 117.01, 21.22; ESI-HRMS *m/z* calcd for $C_{19}H_{17}N_3O_4S$: 406.08320 [M+Na^+], found: 406.08265.

4.6.4. General procedure for synthesis of rhodanine derivatives

Acetic acid (10 mL) was heated to ~80 °C in an oil-bath. The rhodanine derivative (2.5 mmol) and 10 mmol sodium acetate were then added to the hot acid. The mixture was stirred for 5 min before adding 2.5 mmol of the aldehyde. The mixture was then heated to reflux for 16 h, and cooled to room temperature to give in a crystalline product. The mixture was poured into ice-cold water (30 mL) and chilled in an ice-bath for an additional 30 min. The solid was filtered under suction. The crude compounds were then purified by recrystallization with ethanol or a multi-solvent method. The yields ranged from 37% to quantitative. Compounds were characterized by IR, ^1H NMR, ^{13}C NMR, and high resolution ESI-MS.

4.6.4.1. (*Z*)-5-Benzylidene-2-thioxothiazolidin-4-one (4a). Yellow solid; 94% yield: IR (Microscope) 3157, 3064, 2852, 1701, 1445, 1195 cm^{-1}; ^1H NMR (400 MHz, DMSO-d_6): δ = 13.81 (br, 1H), 7.63 (s, 1H), 7.52 (m, 5H); ^{13}C NMR (100 MHz, DMSO-d_6): δ = 196.41, 170.07, 133.66, 132.32, 131.43, 131.16, 130.14, 126.23; EI-HRMS *m/z* calcd for $C_{10}H_7NOS_2$: 220.99690 [M^+], found: 220.99690.

4.6.4.2. (*Z*)-5-(4-Chlorobenzylidene)-2-thioxothiazolidin-4-one (4b). Light yellow solid; 56% yield: IR (Microscope) 3086, 3015, 2852, 1718, 1488, 1188 cm^{-1}; ^1H NMR (400 MHz, DMSO-d_6): δ = 7.61 (s, 1H), 7.58 (d, *J* = 2 Hz, 4H); ^{13}C NMR (100 MHz, DMSO-d_6): δ = 196.11, 170.02, 136.03, 132.74, 132.57, 130.86, 130.20, 127.00; EI-HRMS *m/z* calcd for $C_{10}H_6ClNOS_2$: 254.95793 [M^+], found: 254.95776.

4.6.4.3. (*Z*)-5-(4-(Dimethylamino)benzylidene)-2-thioxothiazolidin-4-one (4c). Red solid; 61% yield: IR (Microscope) 3139, 3042, 2909, 2853, 1682, 1436, 1180 cm^{-1}; ^1H NMR (400 MHz, DMSO-d_6): δ = 13.50 (br, 1H), 7.47 (s, 1H), 7.37 (d, *J* = 8.8 Hz, 2H), 6.77 (d, *J* = 8.8 Hz, 2H), 2.99 (s, 6H); ^{13}C NMR (100 MHz, DMSO-d_6): δ = 195.69, 170.12, 152.44, 133.92, 133.56, 120.45, 118.04, 112.85, 40.26; ESI-HRMS *m/z* calcd for $C_{12}H_{12}N_2OS_2$: 287.02833 [M+Na^+], found: 287.02829.

4.6.4.4. (*Z*)-5-(4-Methoxybenzylidene)-2-thioxothiazolidin-4-one (4d). Yellow solid; 85% yield: IR (Microscope) 3134, 3017, 2934, 2853, 1687, 1446, 1170 cm^{-1}; ^1H NMR (400 MHz, DMSO-d_6): δ = 7.59 (s, 1H), 7.55 (d, *J* = 8.8 Hz, 2H), 7.10 (d, *J* = 8.8 Hz, 2H), 3.82 (s, 3H); ^{13}C NMR (100 MHz, DMSO-d_6): δ = 195.46, 169.39, 161.31, 132.65, 131.85, 125.45, 122.20, 115.06, 55.53; ESI-HRMS *m/z* calcd for $C_{11}H_9NO_2S_2$: 273.99669 [M+Na^+], found: 273.99682.

4.6.4.5. (*Z*)-5-(Naphthalen-1-ylmethylene)-2-thioxothiazolidin-4-one (4e). Light yellow solid; 82% yield: IR (Microscope) 3152, 3056, 3017, 2857, 1691, 1437, 1170 cm^{-1}; ^1H NMR (400 MHz, DMSO-d_6): δ = 8.27 (s, 1H), 8.15 (d, *J* = 8.4 Hz, 1H), 8.07 (dd, *J* = 6.4 Hz, 3.2 Hz, 1H), 8.02 (d, *J* = 8.8 Hz, 1H), 7.65 (m, 4H); ^{13}C NMR (100 MHz, DMSO-d_6): δ = 196.82, 169.48, 133.96, 131.84, 131.72, 130.75, 129.58, 129.45, 128.80, 128.24, 127.56, 127.53, 126.37, 123.99; EI-HRMS *m/z* calcd for $C_{14}H_9NOS_2$: 271. 01254 [M^+], found: 271.01231.

4.6.4.6. (*Z*)-5-(2-Nitrobenzylidene)-2-thioxothiazolidin-4-one (4f). Light green solid; 98% yield: IR (Microscope) 3099, 3033, 2853, 1732, 1533, 1455, 1302, 1200 cm^{-1}; ^1H NMR (400 MHz, DMSO-d_6): δ = 8.16 (dd, *J* = 10.8 Hz, 1.6 Hz, 1H), 7.84 (td, *J* = 10 Hz, 1.6 Hz, 1H), 7.82 (s, 1H), 7.68 (m, 2H); ^{13}C NMR (100 MHz, DMSO-d_6): δ = 196.46, 169.30, 148.65, 135.28, 131.93, 131.03, 130.08, 129.44, 128.53, 126.20; ESI-HRMS *m/z* calcd for $C_{10}H_6N_2O_3S_2$: 288.97121 [M+Na^+], found: 288.97169.

4.6.4.7. (*Z*)-5-(2-Hydroxybenzylidene)-2-thioxothiazolidin-4-one (4g). Orange solid; 76% yield: IR (Microscope) 3496, 3437, 3096, 2846, 1699, 1450, 1163 cm^{-1}; ^1H NMR (400 MHz, DMSO-d_6): δ = 13.66 (br, 1H), 10.62 (s, 1H), 7.83 (s, 1H), 7.28 (m, 2H), 6.94 (m, 2H); ^{13}C NMR (100 MHz, DMSO-d_6): δ = 196.68, 170.19, 158.22, 133.47, 129.94, 127.97, 124.52, 120.63, 120.59, 116.93; ESI-HRMS *m/z* calcd for $C_{10}H_7NO_2S_2$: 259.98104 [M+Na^+], found: 259.98150.

4.6.4.8. (*Z*)-5-Benzylidene-3-ethyl-2-thioxothiazolidin-4-one (5a). Bright yellow solid; 82% yield: IR (dichloromethane cast) 3015, 2982, 2934, 2873, 1705, 1445, 1132 cm^{-1}; ^1H NMR (400 MHz, DMSO-d_6): δ = 7.79 (s, 1H), 7.61 (dt, *J* = 8 Hz, 1.6 Hz, 2H), 7.52 (m, 3H), 4.04 (q, *J* = 7.2 Hz, 2H), 1.17 (t, *J* = 7.2 Hz, 3H); ^{13}C NMR (100 MHz, DMSO-d_6): δ = 193.91, 167.39, 133.69, 133.55, 131.64, 131.32, 130.20, 123.25, 40.17, 12.58; ESI-HRMS *m/z* calcd for $C_{12}H_{11}NOS_2$: 250.03548 [M+H^+], found: 250.03581.

4.6.4.9. (*Z*)-3-Ethyl-5-(2-hydroxybenzylidene)-2-thioxothiazolidin-4-one (5b). Yellow solid; 56% yield: IR (dichloromethane cast) 3256, 3052, 2980, 2916, 2849, 1678, 1456, 1131 cm^{-1}; ^1H NMR (400 MHz, DMSO-d_6): δ = 10.71 (br, 1H), 7.99 (s, 1H), 7.34 (m, 2H), 6.96 (m, 2H), 4.06 (q, *J* = 7.2 Hz, 2H), 1.18 (t, *J* = 7.2 Hz, 3H); ^{13}C NMR (100 MHz, DMSO-d_6): δ = 193.53, 166.84, 157.57, 133.04, 129.57, 128.58, 120.82, 119.97, 119.92, 116.27, 40.17, 11.90; ESI-HRMS *m/z* calcd for $C_{12}H_{11}NO_2S_2$: 288.01234 [M+Na^+], found: 288.01190.

4.6.4.10. (*Z*)-3-Ethyl-5-(4-methoxybenzylidene)-2-thioxothiazolidin-4-one (5c). Bright yellow solid; 53% yield: IR (dichloromethane cast) 3004, 2983, 2961, 2833, 1703, 1457, 1127 cm^{-1}; ^1H NMR (400 MHz, DMSO-d_6): δ = 7.75 (s, 1H), 7.58 (d, *J* = 8.8 Hz, 2H), 7.09 (d, *J* = 8.8 Hz, 2H), 4.03 (q, *J* = 7.2 Hz, 2H), 3.82 (s, 3H), 1.16 (t, *J* = 7.2 Hz, 3H); ^{13}C NMR (100 MHz, DMSO-d_6): δ = 193.65, 167.45, 162.22, 133.83, 133.61, 126.24, 119.86, 115.86, 56.28, 40.17, 12.60; ESI-HRMS *m/z* calcd for $C_{13}H_{13}NO_2S_2$: 280.04605 [M+H^+], found: 280.04675.

4.6.4.11. (*Z*)-5-(4-Chlorobenzylidene)-3-ethyl-2-thioxothiazolidin-4-one (5d). Yellow solid; 79% yield: IR (dichloromethane cast) 3004, 2983, 2971, 2872, 1705, 1433, 1137 cm^{-1}; ^1H NMR (400 MHz, DMSO-d_6): δ = 7.78 (s, 1H), 7.63 (d, *J* = 8.8 Hz, 2H), 7.58 (d, *J* = 8.8 Hz, 2H), 4.03 (q, *J* = 7.2 Hz, 2H), 1.16 (t, *J* = 7.2 Hz, 3H); ^{13}C NMR (100 MHz, DMSO-d_6): δ = 193.61, 167.33, 133.26, 132.90, 132.59, 132.08, 130.26, 124.01, 40.17, 12.56; EI-HRMS *m/z* calcd for $C_{12}H_{10}ClNOS_2$: 282.98923 [M^+], found: 282.98949.

4.6.4.12. (*Z*)-3-Ethyl-5-(naphthalen-1-ylmethylene)-2-thioxothiazolidin-4-one (5e). Yellow-brown solid; 31% yield: IR (dichloromethane cast) 3075, 3055, 2974, 2931, 2873, 1704, 1431, 1133 cm^{-1}; ^1H NMR (400 MHz, $CDCl_3$): δ = 8.49 (s, 1H), 8.16 (d, J = 8.8 Hz, 1H), 7.93 (m, 2H), 7.57 (m, 4H), 4.24 (q, J = 7.2 Hz, 2H), 1.33 (t, J = 7.2 Hz, 3H); ^{13}C NMR (100 MHz, $CDCl_3$): δ = 194.03, 167.38, 133.99, 132.11, 131.66, 130.83, 130.01, 129.26, 127.71, 127.32, 127.05, 126.30, 125.64, 123.62, 40.04, 12.56; EI-HRMS *m/z* calcd for $C_{16}H_{13}NOS_2$: 299.04385 [M^+], found: 299.04404.

4.6.4.13. (*Z*)-3-Ethyl-5-(quinolin-5-ylmethylene)-2-thioxothiazolidin-4-one (5f). Light yellow solid; 40% yield: IR (dichloromethane cast) 3063, 3042, 2978, 2935, 2876, 1712, 1439, 1134 cm^{-1}; ^1H NMR (400 MHz, $CDCl_3$): δ = 9.04 (d, J = 4.4 Hz, 1H), 8.38 (s, 1H), 8.23 (d, J = 8.4 Hz, 1H), 8.16 (d, J = 8.4 Hz, 1H), 7.84 (m, 1H), 7.71 (m, 1H), 7.47 (d, J = 4.8 Hz, 1H), 4.26 (q, J = 7.2 Hz, 2H), 1.36 (t, J = 7.2, 3H); ^{13}C NMR (100 MHz, $CDCl_3$): δ = 192.63, 167.00, 150.03, 148.81, 138.99, 130.67, 130.63, 130.58, 128.12, 126.40, 126.25, 123.52, 119.72, 40.25, 12.52; ESI-HRMS *m/z* calcd for $C_{15}H_{12}N_2OS_2$: 301.04638[M+H^+], found: 301.04641.

4.6.4.14. (*Z*)-3-Amino-5-benzylidene-2-thioxothiazolidin-4-one (6a). Bright yellow solid; 53% yield: IR (dichloromethane cast) 3299, 3225, 3031, 1706, 1448, 1125 cm^{-1}; ^1H NMR (400 MHz, DMSO-d_6): δ = 7.85 (s, 1H), 7.64 (m, 2H), 7.53 (m, 3H), 5.93 (s, 2H); ^{13}C NMR (100 MHz, DMSO-d_6): δ = 187.73, 163.69, 133.31, 132.95, 130.99, 130.70, 129.49, 120.26; ESI-HRMS *m/z* calcd for $C_{10}H_8N_2OS_2$: 258.99703 [M+Na^+], found: 258.99749.

4.6.4.15. (*Z*)-3-Amino-5-(4-methoxybenzylidene)-2-thioxothiazolidin-4-one (6b). Yellow solid; 26% yield: IR (dichloromethane cast) 3288, 3195, 2942, 2842, 1702, 1509, 1131 cm^{-1}; ^1H NMR (400 MHz, DMSO-d_6): δ = 7.76 (s, 1H), 7.57 (d, J = 8.8 Hz, 2H), 7.04 (d, J = 8.8 Hz, 2H), 5.90 (s, 2H), 3.80 (s, 3H); ^{13}C NMR (100 MHz, DMSO-d_6): δ = 187.86, 164.42, 162.27, 134.27, 133.71, 126.23, 117.56, 115.84, 56.28; ESI-HRMS *m/z* calcd for $C_{11}H_{10}N_2O_2S_2$: 289.00759 [M+Na^+], found: 289.00698.

4.6.4.16. (*Z*)-3-Amino-5-(4-chlorobenzylidene)-2-thioxothiazolidin-4-one (6c). Bright yellow solid; 73% yield: IR (dichloromethane cast) 3299, 3234, 3169, 3071, 1727, 1709, 1493, 1128 cm^{-1}; ^1H NMR (400 MHz, DMSO-d_6): δ = 7.83 (s, 1H), 7.65 (d, J = 8.8 Hz, 2H), 7.59 (d, J = 8.8 Hz, 2H), 5.92 (s, 2H); ^{13}C NMR (100 MHz, DMSO-d_6): δ = 188.18, 164.36, 136.34, 133.01, 132.59, 132.56, 130.27, 121.75; ESI-HRMS *m/z* calcd for $C_{10}H_7ClN_2OS_2$: 292.95805 [M+Na^+], found: 292.95793.

4.6.4.17. (*Z*)-*N*-(5-Benzylidene-4-oxo-2-thioxothiazolidin-3-yl)-acetamide (7a). Bright yellow solid; 88% yield: IR (dichloromethane cast) 3192, 3017, 1737, 1679, 1447, 1125 cm^{-1}; ^1H NMR (400 MHz, DMSO-d_6): δ = 7.92 (s, 1H), 7.68 (m, 2H), 7.56 (m, 3H), 2.07 (s, 3H); ^{13}C NMR (100 MHz, DMSO-d_6): δ = 190.54, 167.70, 163.25, 134.58, 132.73, 131.27, 130.80, 129.53, 119.44, 20.28; ESI-HRMS *m/z* calcd for $C_{12}H_{10}N_2O_2S_2$: 301.00759 [M+Na^+], found: 301.00714.

4.6.4.18. (*Z*)-*N*-(5-(4-Methoxybenzylidene)-4-oxo-2-thioxothiazolidin-3-yl)acetamide (7b). Bright yellow solid; 30% yield: IR (dichloromethane cast) 3194, 3013, 2963, 1729, 1679, 1421, 1134 cm^{-1}; ^1H NMR (400 MHz, DMSO-d_6): δ = 11.12 (s, 1H), 7.85 (s, 1H), 7.63 (d, J = 8.8 Hz, 2H), 7.11 (d, J = 8.8 Hz, 2H), 3.83 (s, 3H), 2.05 (s, 3H); ^{13}C NMR (100 MHz, DMSO-d_6): δ = 191.16, 168.36, 164.06, 162.52, 135.48, 133.91, 126.02, 116.67, 115.93, 56.32, 20.99; ESI-HRMS *m/z* calcd for $C_{13}H_{12}N_2O_3S_2$: 331.01815 [M+Na^+], found: 331.01818.

4.6.4.19. (*Z*)-*N*-(5-(4-Chlorobenzylidene)-4-oxo-2-thioxothiazolidin-3-yl)acetamide (7c). Yellow solid; 80% yield: IR (dichloromethane cast) 3199, 3013, 1732, 1680, 1405, 1128 cm^{-1}; ^1H NMR (400 MHz, DMSO-d_6): δ = 7.92 (s, 1H), 7.72 (d, J = 8.5 Hz, 2H), 7.63 (d, J = 8.5 Hz, 2H), 2.07 (s, 3H); ^{13}C NMR (100 MHz, DMSO-d_6): δ = 190.14, 167.56, 163.06, 135.83, 133.11, 132.31, 131.51, 129.50, 120.06, 20.15; ESI-HRMS *m/z* calcd for $C_{12}H_9ClN_2O_2S_2$: 334.96862 [M+Na^+], found: 334.96818.

4.6.4.20. (*Z*)-*N* -(5-((5-(4-Nitrophenyl)furan-2-yl)methylene)-4-oxo-2-thioxothiazolidin-3-yl) acetamide (7d). Orange solid; IR (dichloromethane cast) 3239, 3038, 1729, 1678, 1511, 1139 cm^{-1}; ^1H NMR (400 MHz, DMSO-d_6): δ = 11.14 (s, 1H), 8.37 (d, J = 9.2 Hz, 2H), 8.05 (d, J = 9.2 Hz, 2H), 7.79 (s, 1H), 7.61 (d, J = 4.0 Hz, 1H), 7.44 (d, J = 4.0 Hz, 1H), 2.06 (s, 3H); ^{13}C NMR (100 MHz, DMSO-d_6): δ = 191.77, 168.41, 163.70, 156.51, 151.51, 147.68, 134.81, 126.00, 125.49, 124.28, 120.07, 117.96, 114.55, 20.99; ESI-HRMS *m/z* calcd for $C_{16}H_{11}N_3O_5S_2$: 412.00323 [M+Na^+], found: 412.00278.

Acknowledgments

Financial support was provided by the Natural Sciences and Engineering Research Council of Canada (NSERC), the Alberta Heritage Foundation for Medical Research (AHFMR), and the Canada Research Chair in Bioorganic and Medicinal Chemistry.

References and notes

1. Hutton, C. A.; Perugini, M. A.; Gerrard, J. A. *Mol. BioSyst.* **2007**, *3*, 458–465.
2. Vederas, J. C. *Can. J. Chem.* **2006**, *84*, 1197–1207.
3. Cox, R. J.; Sutherland, A.; Vederas, J. C. *Bioorg. Med. Chem.* **2000**, *8*, 843–871.
4. Scapin, G.; Blanchard, J. S. *Adv. Enzymol.* **1998**, *72*, 279–324.
5. Usha, V.; Dover, L. G.; Roper, D. I.; Fütterer, K.; Besra, G. S. *Acta Crystallogr., Sect. D* **2009**, *65*, 383–387.
6. Pillai, B.; Moorthie, V. A.; van Belkum, M. J.; Marcus, S. L.; Cherney, M. M.; Diaper, C. M.; Vederas, J. C.; James, M. N. G. *J. Mol. Biol.* **2009**, *385*, 580–594.
7. Watanabe, N.; Clay, M. D.; van Belkum, M. J.; Cherney, M. M.; Vederas, J. C.; James, M. N. G. *J. Mol. Biol.* **2008**, *384*, 1314–1329.
8. Kefala, G.; Evans, G. L.; Griffin, M. D. W.; Devenish, S. R. A.; Pearce, F. G.; Perugini, M. A.; Gerrard, J. A.; Weiss, M. S.; Dobson, R. C. J. *Biochem. J.* **2008**, *411*, 351–360.
9. Hu, T.; Wu, D.; Chen, J.; Ding, J.; Jiang, H.; Shen, X. *J. Biol. Chem.* **2008**, *283*, 21284–21293.
10. Nguyen, L.; Kozlov, G.; Gehring, K. *FEBS Lett.* **2008**, *582*, 623–626.
11. Weyand, S.; Kefala, G.; Weiss, M. S. *J. Mol. Biol.* **2007**, *367*, 825–838.
12. Gillner, D.; Armoush, N.; Holz, R. C.; Becker, D. P. *Bioorg. Med. Chem. Lett.* **2009**, *19*, 6350–6352.
13. Paradis-Bleau, C.; Lloyd, A.; Sanschagrin, F.; Maaroufi, H.; Clarke, T.; Blewett, A.; Dowson, C.; Roper, D. I.; Bugg, T. D. H.; Levesque, R. C. *Biochem. J.* **2009**, *421*, 263–272.
14. Boughton, B. A.; Dobson, R. C. J.; Gerrard, J. A.; Hutton, C. A. *Bioorg. Med. Chem. Lett.* **2008**, *18*, 460–463.
15. Boughton, B. A.; Griffin, M. D. W.; O'Donnell, P. A.; Dobson, R. C. J.; Perugini, M. A.; Gerrard, J. A.; Hutton, C. A. *Bioorg. Med. Chem.* **2008**, *16*, 9975–9983.
16. Kelland, J. G.; Arnold, L. D.; Palcic, M. M.; Pickard, M. A.; Vederas, J. C. *J. Biol. Chem.* **1986**, *261*, 13216–13223.
17. Mazur, B.; Krebbers, E.; Tingey, S. *Science* **1999**, *285*, 372–375.
18. Pillai, B.; Cherney, M. M.; Diaper, C. M.; Sutherland, A.; Blanchard, J. S.; Vederas, J. C.; James, M. N. G. *Biochem. Biophys. Res. Commun.* **2007**, *363*, 547–553.
19. Pillai, B.; Cherney, M. M.; Diaper, C. M.; Sutherland, A.; Blanchard, J. S.; Vederas, J. C.; James, M. N. G. *Proc. Natl. Acad. Sci. U.S.A.* **2006**, *103*, 8668–8673.
20. Hudson, A. O.; Singh, B. K.; Leustek, T.; Gilvarg, C. *Plant Physiol.* **2006**, *140*, 292–301.
21. Kelland, J. G.; Palcic, M. M.; Pickard, M. A.; Vederas, J. C. *Biochemistry* **1985**, *24*, 3263–3267.
22. Watanabe, N.; Cherney, M. M.; van Belkum, M. J.; Marcus, S. L.; Flegel, M. D.; Clay, M. D.; Deyholos, M. K.; Vederas, J. C.; James, M. N. *J. Mol. Biol.* **2007**, *371*, 685–702.
23. McCoy, A. J.; Adams, N. E.; Hudson, A. O.; Gilvarg, C.; Leustek, T.; Maurelli, A. T. *Proc. Natl. Acad. Sci. U.S.A.* **2006**, *103*, 17909–17914.

24. Hudson, A. O.; Gilvarg, C.; Leustek, T. *J. Bacteriol.* **2008**, *190*, 3256–3263.
25. Graham, D. E.; Huse, H. K. *FEBS Lett.* **2008**, *582*, 1369–1374.
26. Cox, R. J.; Wang, P. S. H. *J. Chem. Soc., Perkin Trans. 1* **2001**, 2022–2034.
27. *Martindale: the Complete Drug Reference*; Sweetman, S. C., Ed., 34th ed.; Pharmaceutical Press: London, 2005; pp 222–224.
28. Haldar, M. K.; Scott, M. D.; Sule, N.; Srivastava, D. K.; Mallik, S. *Bioorg. Med. Chem. Lett.* **2008**, *18*, 2373–2376.
29. (a) Hutchings, S.; Liu, W.; Radinov, R. *Heterocycles* **2006**, *67*, 763; (b) Kim, S. H.; Pudzianowski, A. T.; Leavitt, K. J.; Barbosa, J.; McDonnell, P. A.; Metzler, W. J.; Rankin, B. M.; Liu, R.; Vaccaro, W.; Pitts, W. *Bioorg. Med. Chem. Lett.* **2005**, *15*, 1101–1106; (c) Daniewski, A. R.; Liu, W.; Okabe, M. *Org. Proc. Res. Dev.* **2004**, *8*, 411; (d) Suzuki, H.; Kneller, M. B.; Rock, D. A.; Jones, J. P.; Trager, W. F.; Rettie, A. E. *Arch. Biochem. Biophys.* **2004**, *429*, 1; (e) Soong, C. L.; Ogawa, J.; Sakuradani, E.; Shimizu, S. *J. Biol. Chem.* **2002**, *277*, 7051.
30. Segel, I. H. *Enzyme Kinetics*; John Wiley & Sons: New York, 1993.